

Strontium Optical Lattice Clock at JILA

M. Boyd, A. Ludlow, S. Foreman, T. Zelevinsky, S. Blatt, T. Zanon, G. Campbell, M. Miranda, M. Martin, and J. Ye
JILA, National Institute of Standards and Technology and University of Colorado, Department of Physics,
University of Colorado, Boulder, CO 80309-0440, USA
boydmm@colorado.edu

Abstract—Recent results from the JILA optical lattice clock are presented. We report on our development of precision tools for the lattice clock, including a stabilized clock laser with sub-Hz linewidth, fs-comb based technology allowing accurate clock comparison in both the microwave and optical domains, and clock transfer over optical fiber in an urban environment. High resolution spectroscopy ($Q > 2 \times 10^{14}$) of lattice confined strontium atoms is used for both a high-performance optical clock and atomic structure measurements. The current accuracy and stability of the lattice clock are also discussed.

I. INTRODUCTION

The major motivation behind the development of optical atomic clocks is the enhanced measurement precision resulting from the large line quality factors (Q) which now exceed 10^{14} [1, 2]. The lattice clock technique [3-7] presents an intriguing situation in which one can benefit from the large signal to noise ratio (S/N) provided by a neutral atom ensemble, while enjoying many of the spectroscopic features of trapped ions. The lattice potential provides Lamb-Dicke confinement where the resonance feature of interest is not influenced by atomic motion, enabling high precision, high accuracy measurements.

The weakly allowed 1S_0 - 3P_0 transition in alkaline-earth(-like) atoms is particularly well suited for such a scheme due to the existence of a magic wavelength where the ac Stark shift from the trapping laser is identical for the two clock states, and the insensitivity of the states to lattice polarization. The accuracy of a lattice clock based on ^{87}Sr is expected to reach below 10^{-17} , while the stability could reach below 10^{-16} at 1 s for a sufficiently pre-stabilized laser. Such lofty accuracy and precision goals will require focused technical efforts in both laser development and precision spectroscopy. In this paper we report the present status of our clock system, including local oscillator performance, clock comparison technology using fs-combs, high resolution spectroscopy, and the current level of accuracy and stability of the lattice clock.

II. OPTICAL CLOCKWORK

A. Stable Local Oscillator

For the purposes of operating a clock with the best possible stability, it is necessary for the probe laser to have

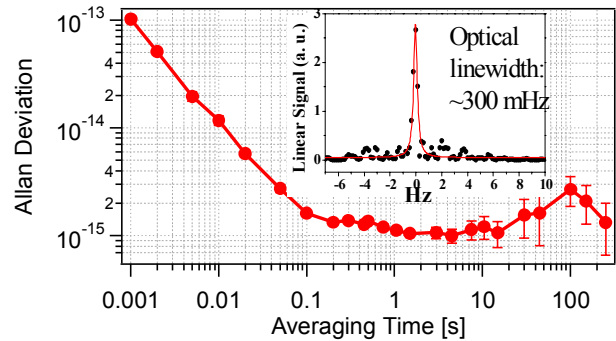


Figure 1. Allan deviation (with linear drift removed) for a heterodyne beat between two independent clock laser systems at 698 nm. The 1×10^{-15} stability at 1 s is consistent with the estimated thermal noise limit. The inset shows the beat between the lasers is well below 1 Hz for an integration time of a few seconds.

both a narrow intrinsic linewidth as well as small frequency drift and low instability. Development of such an oscillator to probe the Sr clock transition at 698 nm has therefore been one of the central focuses of our work. The stabilization scheme for our laser is discussed in detail elsewhere [8]. Briefly, a grating-stabilized diode laser is locked to a high-finesse ultra-low-expansion (ULE) cavity mounted in a vertical orientation in order to reduce fluctuations of the cavity length due to vibrations [9]. The cavity is under vacuum and mounted on a compact, passive vibration-isolation table.

The clock laser performance has been characterized in a number of ways, including direct comparison of two similar systems at 698 nm, comparison to highly stabilized lasers at other colors using the fs-comb (discussed in section II B), and by precision atomic spectroscopy (discussed in section III). Direct comparison between the two 698nm systems via heterodyne beat reveals narrow linewidths often below 300 mHz for integration times of a few seconds, as shown in the inset of Fig. 1. The Allan deviation shown in Fig. 1 reveals that the fractional frequency noise of the beat is $\sim 1 \times 10^{-15}$ at 1 s, consistent with the expected limit set by thermal-mechanical noise in the cavity mirrors and mirror coatings [10].

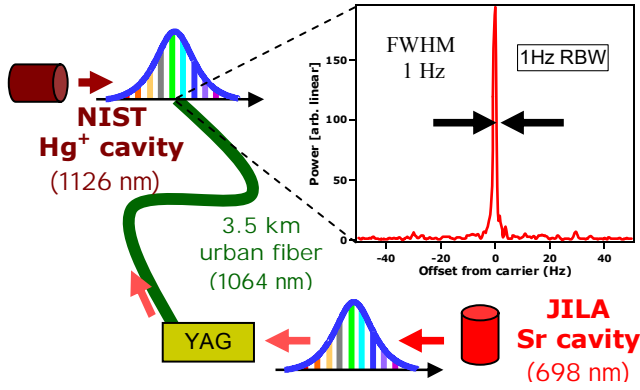


Figure 2. Optical beat between the fiber transfer laser and the NIST comb at 1064 nm. The fs-comb in JILA is stabilized to the 698 nm clock laser transferring the stability across the optical spectrum. A 1064 nm Nd:YAG laser is stabilized to the comb and used as a transfer laser to send clock information to NIST over a 3.5 km fiber which is optical phase stabilized. At NIST, a second fs-comb stabilized to the 1126 nm Hg^+ clock laser is used to compare the two stable oscillators. The beat between the NIST comb and the transfer laser is 1 Hz wide, limited by the resolution bandwidth of the measurement.

B. fs-comb Clockwork and Precision Fiber Transfer

The fs-comb in our lab plays an essential role for clock development as it provides a coherent link between high accuracy clocks operating in either the optical or microwave domains. For absolute frequency measurements, a direct-octave-spanning frequency comb similar to that reported in [11] is locked to the probe laser at 698 nm, and is also self-referenced. The comb provides a measurement of the laser frequency relative to a microwave signal derived from a hydrogen maser calibrated to the NIST primary Cs fountain clock [12]. To enable the microwave comparison, a diode laser operating near 1320 nm is amplitude-modulated and transmitted over a 3.5-km fiber optic link from NIST to our lab [13, 14]. The instability of the frequency-counting signal is $\sim 2.5 \times 10^{-13}$ for a 1-s integration time. Transfer of the microwave reference over the urban fiber does require caution as periodic stretching and compressing of the fiber, associated with daily temperature cycles, has been found to cause frequency offsets as large as 10^{-14} . Stabilization of the fiber link is therefore essential for high accuracy clock comparisons [14].

The comb and fiber link also supports transmission of stable optical frequencies between our lab and NIST. While the fiber link does not allow transfer of the 698 nm light, the comb can be used to transfer the clock stability across the optical spectrum allowing use of a transfer laser at 1064 nm. We have examined the precision of the transfer across the comb spectrum by comparing our 698 nm clock laser with a similar independent system operating at 1064 nm [9]. The resulting beat between the stabilized comb and the 1064 nm laser has a linewidth below 0.5 Hz, verifying the ability of the comb to preserve the narrow linewidth provided by the 698 nm laser. For transfer of our clock signal, a 1064 nm laser is locked to the comb and transferred through the fiber to the NIST laboratory where it can be measured relative to a number of high accuracy optical clocks [15, 16, 7] using a second fs-comb. To eliminate noise induced by the transfer,

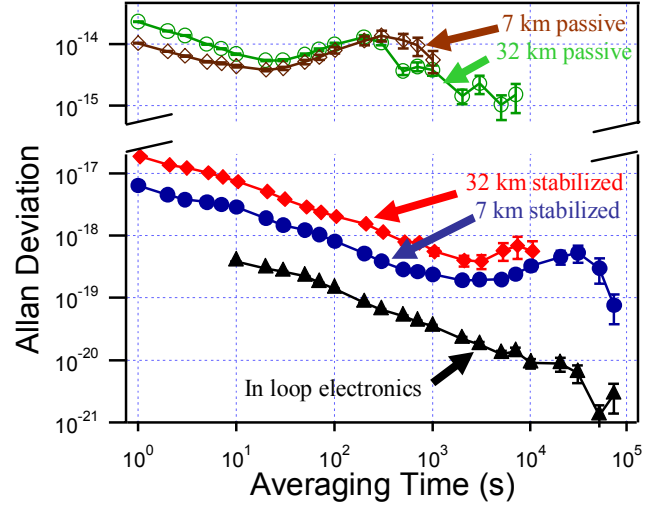


Figure 3. Allan deviations (in fractional frequency units) showing the stability of the fiber transfer system for both passive (open data) and stabilized (closed data) fiber links. Data is shown for both the 7 km round trip length between JILA and NIST, and a longer length of 32 km.

the 1064 nm light is partially reflected back to our lab allowing interferometrical stabilization of the link [17]. Fig. 2 shows a beat between the transfer laser and a fs-comb on the NIST end which is stabilized to the local oscillator used for the Hg^+ clock [18]. The beat has a resolution-bandwidth-limited linewidth of 1 Hz, demonstrating that the phase coherence of the two clock lasers is not degraded by the two fs-combs and the fiber transfer process. In addition, Fig. 3 summarizes characterizations of passive and phase-stabilized optical transfer for 7 km (the round trip length of our fiber link) and 32 km fiber lengths. For the 7 km length typically used for clock experiments, the transfer noise is at the 1×10^{-17} level at 1 s [17].

III. HIGH RESOLUTION SPECTROSCOPY

With the oscillator and clockwork in place, our attention turns to the development of an accurate atomic reference using lattice confined neutral strontium. ^{87}Sr atoms are laser cooled in two stages [19, 4], using a combination of broad (32 MHz) and narrow (7.4 kHz) cycling transitions. During the cooling a vertical one-dimensional lattice is overlapped with the atomic cloud. When the cooling light is extinguished, roughly 10^4 atoms remain trapped in the lattice, at a temperature of ~ 2 μK , ready for interrogation.

A. Spectroscopy of Confined Atoms

The lattice potential is sufficiently deep such that the $^1\text{S}_0$ - $^3\text{P}_0$ clock transition is probed in the Lamb-Dicke regime where the spatial dimension of the confinement is small compared to the interrogation wavelength. The resulting absorption spectrum is free of Doppler or recoil effects, allowing high line Q's to be achieved. When the transition is strongly saturated, spectra such as that in Fig. 4 (a) are observed. Here the narrow transition is accompanied by motional sidebands.

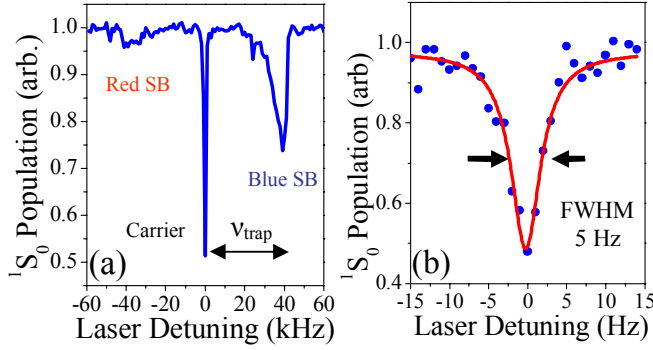


Figure 4. High resolution spectroscopy of lattice confined Sr atoms. (a) Resolved longitudinal sideband (SB) spectrum observed when the transition is strongly saturated. The trap frequency is determined from the position of the red and blue sidebands relative to the carrier (clock) transition. The atom temperature can be extracted from the lineshape of the sidebands which are asymmetrically broadened due to motion in the trap. (b) The narrow carrier transition used as the atomic reference. Here the 5 Hz linewidth is limited by residual magnetic fields.

The sideband spectrum is useful for direct measurement of the thermal-mechanical properties of the trapped atoms including temperatures and trap motional frequencies [4]. The narrow central feature is of most interest to us as an atomic reference as it is the absorption feature which does not include any motional or Stark broadening when the magic wavelength condition is achieved. In the unsaturated case, this ‘carrier’ transition has a width of only 5 Hz, as showing in figure 4(b), which represents a line Q of nearly 10^{14} .

B. Nuclear Spin Effects

The limit to the achievable line Q in Fig. 4(b) is mainly due to magnetic sensitivity of the clock transition. The hyperfine state mixing mechanism, which results in the ~ 1 mHz linewidth of the otherwise forbidden clock transition, increases the magnetic moment of the 3P_0 state, resulting in a small differential g-factor between 3P_0 and 1S_0 . The resultant sensitivity of the clock transition to external magnetic fields requires careful consideration for clock development to ensure the frequency is accurate and stable.

To explore the magnitude of the differential g-factor we have performed NMR-like measurements on various m_F -sublevels of the clock transition in the presence of a bias magnetic field. Fig. 5(a) shows the absorption spectrum in the presence of a bias field using linearly polarized light to drive the ten possible π -transitions ($\Delta m_F = 0$). In Fig. 5(b) the probe light polarization is rotated by 90 degrees from the quantization axis such that nine σ^- ($\Delta m_F = -1$) and nine σ^+ ($\Delta m_F = +1$) transitions are observed simultaneously. While the π -transitions would be sufficient for measurement of the differential g-factor magnitude, the σ^{\pm} transitions provide more information as the spectrum depends on both the magnitude of the effect and the sign (i.e. the state mixing *increases* the 3P_0 g-factor). Furthermore, calibration of the field magnitude is automatic if the ground state magnetic moment is known. Spectroscopy of the resolved sublevels has

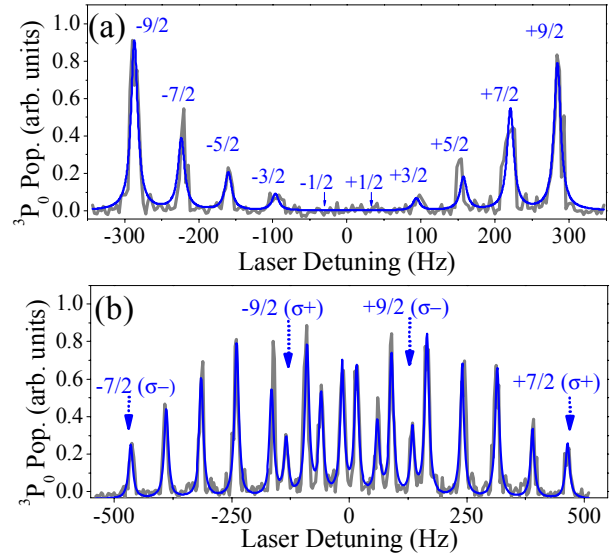


Figure 5. Spectroscopy of resolved m_F -sublevels in the presence of a magnetic bias field. (a) Ten π -transitions are observed when the probe is linearly polarized along the quantization axis set by the 0.58 G magnetic field. (b) When the probe polarization is orthogonal to the quantization axis 18 σ transitions are seen, in the case with a bias field of 0.69 G. In both (a) and (b) peaks are labeled according to the ground state m_F origin of the transition. In (b) the spectrum consists of two overlapped sets of nine evenly spaced peaks, the excitation polarization is labeled to aid the eye.

allowed precise measurement of the differential g-factor yielding $108.4(4) \times m_F \text{ Hz/G}$ (where $G = 10^{-4} \text{ T}$) [20, 1]. The resolved spectrum has also allowed experimental investigation of the tensor light shift sensitivity of the clock states, demonstrating that they should have a minimal impact on the 1-D lattice clock [20].

C. Hz-level Optical Spectroscopy

With the degeneracy of the clock states lifted in the presence of a magnetic field, the resolved transitions can be explored free of broadening from state dependent Zeeman and Stark shifts, revealing the true spectroscopic limit of our system. An example of this is shown in Fig. 5(a) where the 3P_0 ($m_F = 5/2$) population is measured as the laser is tuned across the resonance. The resulting resonance width in this case is $2.1(2) \text{ Hz}$ ($Q \sim 2 \times 10^{14}$) [1], near the $\sim 1.8 \text{ Hz}$ Fourier limit set by the 500ms interrogation time. Laser frequency noise prevents us from going to longer probe times as the beat between our two 698 nm lasers, discussed in Section IIA broadens to nearly 2 Hz when integrated over the relevant timescale for scanning the line (about 30 s). Ramsey spectroscopy can also be performed, as shown in Fig. 5(b). The Doppler-free absorption spectrum and long interaction time provided by the lattice confinement allows use of long, low intensity pulses for the Ramsey sequence, resulting in simple spectra with a small number of fringes. This has simplified the identification of the central fringe compared to that of free falling clouds of cold atoms.

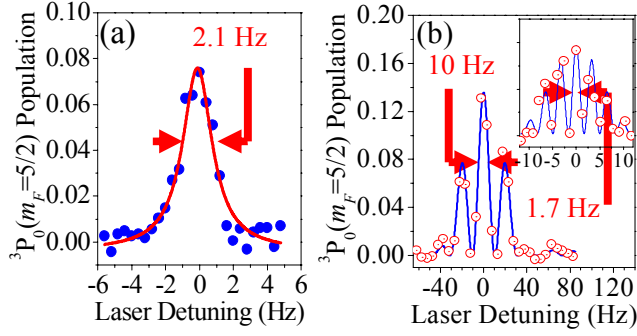


Figure 6. High resolution spectroscopy of the $m_F=5/2$ sublevel. (a) Ultra-narrow ($Q>2\times 10^{14}$) spectrum achieved with a 500 ms Rabi pulse. (b) Ramsey spectrum for 25 ms Ramsey pulses separated by a 80 ms dark time resulting in a 10 Hz FWHM for the central fringe. The inset shows the spectrum for longer pulse and dark times of 80 ms and 200 ms respectively. In both (a) and the inset of (b) the Q is limited by laser frequency noise during the ~ 30 s acquisition time for each lineshape.

IV. CLOCK PERFORMANCE

The high-resolution spectroscopy presented in the previous sections gives confidence in the lattice clock technique as a tool for precision measurement. The high stability oscillator, large line Q , and relatively large S/N can result in clock stability at the 2×10^{-15} level at 1 s. A remaining issue is the level of accuracy that can be achieved with the lattice system.

A. Accuracy Evaluation (2006): Degenerate Sublevels

We first present our recent accuracy evaluation using degenerate sublevels, that is, operating the lattice clock without a bias magnetic field. To evaluate the accuracy of the ^{87}Sr lattice clock we used an interleaved scheme where the parameters of interest were quickly varied during a scan of the transition, allowing us to extract the shift coefficient using the precision of the laser cavity as a reference. In this way, we explored a variety of systematic effects, with dominant contributions to our uncertainty budget being the lattice shift, density shift, and Zeeman shift. Operating at a lattice wavelength of 813.4280(5) nm, we found that the ac Stark shift for our typical trap depth was $-2.5(6.0)\times 10^{-16}$. For our typical density of $\sim 5\times 10^{11}\text{ cm}^{-3}$, the collision shift was constrained to be below 3.3×10^{-16} . Each of these effects was consistent with zero and limited by the statistical uncertainty associated with hundreds of measurements. The Zeeman sensitivity was found to be non-zero but less than 5.3×10^{-16} when the residual magnetic field was controlled to 5 mG. Due to the differential g-factor, we could zero and monitor the field to this level using the transition linewidth. The total uncertainty for lattice spectroscopy under our operating conditions was 9×10^{-16} [5].

With the spectroscopy systematics well under control, an absolute frequency measurement was performed using the fiber link and H-maser system discussed above. After a 24 hour run of measurements, the frequency of the $^{87}\text{Sr } 1S_0-3P_0$ transition frequency was found to be 429,228,004,229,874.0 ± 1.1 Hz. The total uncertainty of 2.5×10^{-15} was dominated by the statistical uncertainty in the comparison (1.4×10^{-15}), and the maser calibration (1.7×10^{-15}) [5]. Fig. 7 summarizes the

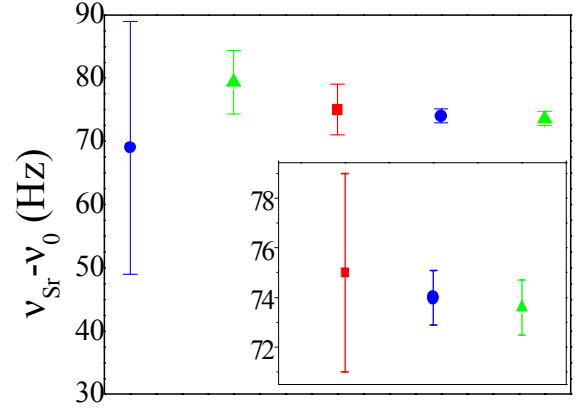


Figure 7. Recent absolute frequency measurements of the ^{87}Sr clock transition by JILA (blue circles), Paris (green triangles), and Tokyo (red squares). The frequency is reported relative to a reference frequency $\nu_0=429,228,004,229,800$ Hz. The inset shows a close up view of the last three points on the main plot. Note that the last two [5, 21] differ by only 9×10^{-16} .

recent absolute frequency measurements made by our group at JILA [4, 5], and the groups in Paris [6, 21] and Tokyo [22]. The excellent agreement between independent groups speaks strongly for the ^{87}Sr lattice clock as a frequency standard.

B. Accuracy Evaluation (in progress) : Spin-Polarized Samples

The systematic uncertainties associated with lattice spectroscopy discussed above were for the most part limited by the statistical uncertainty of the measurement. The magnetic field sensitivity on the other hand was limited by the field calibration and is of some concern. To avoid shift due to the linear Zeeman shift, our current setup now employs spin-polarized samples where the atoms are optically pumped to the $m_F = \pm 9/2$ states before spectroscopy. In this situation spectroscopy is performed in the presence of a small bias field and the positions of the two resonances are used to determine the mean frequency which is independent of the magnetic bias field. The high resolution discussed above allows us to operate in this mode with a small bias field making the second order Zeeman shift negligible [20].

With the main concern in the uncertainty budget now eliminated, the remaining terms can be reduced further by decreasing the statistical uncertainty of the shifts. To improve the precision of our evaluation, we have begun comparing the JILA Sr clock against a high-precision Ca optical clock at NIST [15] using the fiber link discussed above. Fig. 8 shows the results of a clock comparison between the spin-polarized ^{87}Sr lattice clock and the Ca clock. The stability at 1 s is $\sim 3\times 10^{-15}$ and a precision of 3×10^{-16} is achieved in only 200 seconds of averaging. With the combination of increased precision and the spin-polarized method, it is expected that the systematic uncertainty of our lattice clock will be reduced to the 1×10^{-16} level.

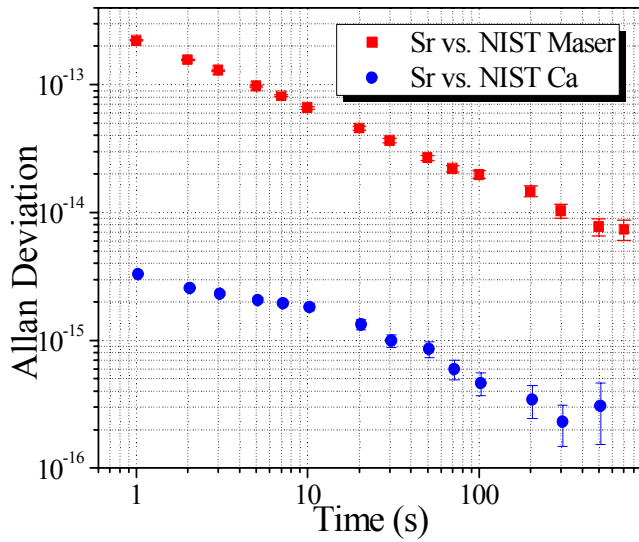


Figure 8. Microwave and optical clock comparisons using the fiber link discussed in the text. The allan deviation for the Sr-Maser comparison is shown as red squares yielding a stability of $\sim 2.5 \times 10^{-13} \tau^{-1/2}$. The advantage of an optical clock is obvious from the Sr-Ca comparison which typically yields stability of $< 5 \times 10^{-15} \tau^{-1/2}$.

V. CONCLUSION

We have presented our recent results towards developing an optical frequency standard based on strontium atoms confined in an optical lattice. The local oscillator is now performing at the 1×10^{-15} level at 1-1000 s, and the fiber/comb transfer system has been shown to support precision frequency transfer at the level of 1×10^{-17} at 1 s. The lattice clock technique, combined with the high precision laser, has yielded the highest line Q ($> 2 \times 10^{14}$) achieved in coherent spectroscopy, with a good S/N for further enhanced stability. Nuclear-spin effects in the lattice clock have been explored, including a measurement of the differential g-factor of the clock transition. An accuracy evaluation was performed, reducing the lattice clock systematics below 10^{-15} , and an absolute frequency measurement with a 1 Hz uncertainty was made, which is in excellent agreement with that of other groups. Comparison of the Sr clock with the NIST Ca clock revealed the clock instability is less than $5 \times 10^{-15} \tau^{-1/2}$. Using the high precision optical comparison and spin polarized samples the lattice clock systematics are expected to reach the 1×10^{-16} level in the near future.

ACKNOWLEDGMENTS

We gratefully acknowledge contributions from the NIST Time and Frequency Division. We thank Z. Barber, J. Bergquist, S. Diddams, T. Fortier, L. Hollberg, C. Oates, T. Parker, and J. Stalnaker for help with a number of projects presented here including the fiber-link based laser comparison, Sr - Ca optical clock comparison, and the absolute frequency measurements made via the Sr - maser comparison.

REFERENCES

- [1] M. M. Boyd et al., "Optical atomic coherence at the 1-second time scale," *Science*, vol. 314, pp. 1430-1433, 2006.
- [2] R. J. Rafac, B. C. Young, J. A. Beall, W. M. Itano, D. J. Wineland, and J. C. Bergquist, "Sub-dekahertz ultraviolet spectroscopy of $^{199}\text{Hg}^+$," *Phys. Rev. Lett.*, vol. 85, p. 2462, 2000.
- [3] M. Takamoto, F.-L. Hong, R. Higashi, and H. Katori, "An optical lattice clock," *Nature*, vol. 435, pp. 321-324, 2005.
- [4] A. D. Ludlow et al., "Systematic study of the ^{87}Sr clock transition in an optical lattice," *Phys. Rev. Lett.*, vol. 96, p. 033003, 2006.
- [5] M. M. Boyd et al., " ^{87}Sr lattice clock with inaccuracy below 10^{-15} ," *Phys. Rev. Lett.*, vol. 98, p. 083002, 2007.
- [6] R. Le Targat et al., "Accurate optical lattice clock with ^{87}Sr atoms," *Phys. Rev. Lett.*, vol. 97, p. 130801, 2006.
- [7] Z. W. Barber, C. W. Hoyt, C. W. Oates, L. Hollberg, A. V. Taichenachev, and V. I. Yudin, "Direct excitation of the forbidden clock transition in neutral ^{174}Yb atoms confined to an optical lattice," *Phys. Rev. Lett.*, vol. 96, p. 083002, 2006.
- [8] A. D. Ludlow et al., "Compact, thermal-noise-limited optical cavity for diode laser stabilization at 1×10^{-15} ," *Opt. Lett.*, vol. 32, pp. 641-643, 2007.
- [9] M. Notcutt, L.-S. Ma, J. Ye, and J. L. Hall, "Simple and compact 1-Hz laser system via an improved mounting configuration of a reference cavity," *Opt. Lett.*, vol. 30, pp. 1815-1817, 2005.
- [10] K. Numata, A. Kemery, and J. Camp, "Thermal-noise limit in the frequency stabilization of lasers with rigid cavities," *Phys. Rev. Lett.*, vol. 93, p. 250602, 2004.
- [11] T. M. Fortier, D. J. Jones, and S. T. Cundiff, "Phase stabilization of an octave-spanning Ti:sapphire laser," *Opt. Lett.*, vol. 28, pp. 2198-2200, 2003.
- [12] T. P. Heavner, S. R. Jefferts, E. A. Donley, J. H. Shirley, and T. E. Parker, "NIST-F1: recent improvements and accuracy evaluations," *Metrologia*, vol. 42, p. 411, 2005.
- [13] J. Ye et al., "Delivery of high-stability optical and microwave frequency standards over an optical fiber network," *JOSA B*, vol. 20, pp. 1459-1467, 2003.
- [14] S. M. Foreman, K. W. Holman, D. D. Hudson, D. J. Jones, and J. Ye, "Remote transfer of ultrastable frequency references via fiber networks," *Rev. Sci. Instrum.*, vol. 78, p. 021101, 2007.
- [15] G. Wilpers, C. W. Oates, and L. Hollberg, "Improved uncertainty budget for optical frequency measurements with microkelvin neutral atoms: results for a high-stability ^{40}Ca optical frequency standard," *Appl. Phys. B*, vol. 85, pp. 31-44, 2006.
- [16] W. H. Oskay et al., "Single atom optical clock with high accuracy," *Phys. Rev. Lett.*, vol. 97, p. 020801, 2006.
- [17] S. M. Foreman et al., "Coherent optical phase transfer over a 32-km fiber with long-term instability $< 10^{-18}$," unpublished, 2007.
- [18] B. C. Young, F. C. Cruz, W. M. Itano, and J. C. Bergquist, "Visible lasers with subhertz linewidths," *Phys. Rev. Lett.*, vol. 82, p. 3799, 1999.
- [19] T. Loftus, T. Ido, A. D. Ludlow, M. M. Boyd, and J. Ye, "Narrow line cooling: finite photon recoil dynamics," *Phys. Rev. Lett.*, vol. 93, p. 073003, 2004; T. Loftus, T. Ido, M. M. Boyd, A. D. Ludlow, and J. Ye, "Narrow line cooling and momentum-space crystals," *Phys. Rev. A*, vol. 70, p. 063413, 2004.
- [20] M. M. Boyd et al., "Nuclear spin effects in optical lattice clocks," *Phys. Rev. A*, in press, 2007. Also available at arxiv:0704.0912v1.
- [21] P. Lemonde et al., "An optical lattice clock with spin-polarized ^{87}Sr atoms," *Proceedings of the Joint 2007 European Frequency and Time Forum & 2007 IEEE Frequency Control Symposium*, Geneva, Switzerland, May 28th-June 1st, 2007.
- [22] M. Takamoto, F.-L. Hong, R. Higashi, Y. Fujii, M. Imae, and H. Katori, "Improved frequency measurement of a one-dimensional optical lattice clock with a spin-polarized fermionic ^{87}Sr isotope," *J. Phys. Soc. Japan*, vol. 75, p. 104302, 2006.